



# Validation of Soil Thermal Conductivity Models

Gerd Wessolek<sup>1</sup> · Klaus Bohne<sup>2</sup> · Steffen Trinks<sup>1</sup>

Received: 27 July 2022 / Accepted: 18 October 2022 / Published online: 2 December 2022  
© The Author(s) 2022

## Abstract

This study describes the generation of a uniform data base of 2733 non-stationary thermal conductivity laboratory measurements of about 158 soil cores with varying texture, bulk density, soil organic matter, pH, and carbonate content. This data set has been used to validate ten well established pedo-transfer functions for predicting thermal conductivity by using easily available soil information such as soil texture, bulk density, and water content. Models were grouped into (i) physically based and (ii) empirical ones that need measured data for its calibration. The classical physical based transfer-function of deVries et al. has been finally chosen to set up a framework of standard values for the USDA soil classes. For planning purposes, these  $\lambda$  estimates for selected pressure heads only need information on soil texture and bulk density and may be more valuable than single point values of thermal conductivity.

**Keywords**  $\lambda$ -Frame for USDA soil texture classes ·  $\lambda$ -Pedotransfer functions · Laboratory measurements · Model-validation · Prediction of soil thermal conductivity · Soil thermal conductivity

## Abbreviations

- $\lambda$  Thermal conductivity,  $\text{W}\cdot\text{m}^{-1}\cdot\text{K}^{-1}$   
 $\lambda_w$  Thermal conductivity of water:  $0.57\text{ W}\cdot\text{m}^{-1}\cdot\text{K}^{-1}$   
 $\rho_p$  Particle density,  $\text{g}\cdot\text{cm}^{-3}$   
 $\rho_b$  Bulk density,  $\text{g}\cdot\text{cm}^{-3}$   
 $\Phi$  Porosity ( $\text{cm}^3\cdot\text{cm}^{-3}$ ), given by  $\Phi = 1 - \rho_b/\rho_p$

---

✉ Gerd Wessolek  
gerd.wessolek@tu-berlin.de

Klaus Bohne  
klaus.bohne@uni-rostock.de

Steffen Trinks  
steffen.trinks@tu-berlin.de

<sup>1</sup> Institute of Ecology, Technische Universität Berlin, Ernst Reuter Platz 1, 10587 Berlin, Germany

<sup>2</sup> Institute of Soil Science, Universität Rostock, Justus-Von-Liebig-Weg 6, 18051 Rostock, Germany

- $\theta$  Volumetric water content,  $\text{cm}^3 \cdot \text{cm}^{-3}$   
S Saturation degree, given by  $S = \theta/\nu$

## 1 Introduction

In geosciences and geotechnical disciplines, one observes an increasing demand for the thermal conductivity characteristics of soils covering the full range of texture, bulk density, and water content. Reasons for this requirement are (i) tasks and challenges connected with modeling climate change effects on the energy, water, and heat balance of landscapes, (ii) problems in designing and finding save landfill liners, (iii) ecological and agricultural claims against energy companies planning underground cable liners, and (iv) an increasing demand of geothermal heat as an energy resource for heating buildings. Thus, a series of technical and environmentally relevant questions need to be answered on how soil heat balance and temperatures are changing.

The main target for a landfill liner is to avoid a long-term drying out process of a clay-layer beneath a waste disposal. Water vapor losses might occur caused by temperature gradients from the warming waste inside to the colder outside [1–3].

When underground cables are in use, they generate heat due to the resistance of the electric power transport. To maintain the cables' capacity and extend their lifetime, it is important for the heat to be dissipated as efficiently as possible into the surrounding soil in order to avoid cables from overheating [4–6]. Heat dissipation from the cable into the surrounding soil depends on ambient conditions such as the site's climate, soil physical properties, usage, and groundwater level. However, it is well known since many years (Brakelmann, 1984, Campbell et al. 2010): The key factor is the thermal conductivity of the surrounding soil [7, 8].

For some of these examples it is essential to know the thermal conductivity not only for a certain point in the landscape, but for large regions or for extreme long cable routes, which often are designed for thousands of miles. Especially in the planning phase, there is an urgent need for calibrated models and parameter to predict the thermal conductivity for the whole cable transect in order to optimize the technique [9].

Many papers, such as Dong et al., Tarnawski et al., and He et al. have been published testing and comparing various models to predict the thermal conductivity of soils [10–12]. To our knowledge, no paper exists that only uses standardized measured data gained by the same lab equipment and method to validate various pedo-transfer-models. In this paper, we provide and use such a standardized data set ( $n=2733$  data points) for validating ten well described and established pedotransfer-transfer functions. We selected those, which have been qualified by He et al., the as "best performing" models [12].

Based upon the best performing functions, we generated guideline values for the USDA- soil textural classes for selected values of bulk density and water content.

## 2 Generation of a Standardized Thermal Conductivity Data Base

For this study, we only consider thermal conductivity data that have been gained by a non-stationary laboratory method, which uses the so-called heat impulse method as suggested by DeVries [13]. Because the laboratory method and procedure has been already introduced in detail by Trinks [14], and tested by Markert et al., we only briefly describe the device and measuring technique [15, 16]. In the second part of this chapter, information is given on the soil data base used for the validation of the pedo-transfer-functions.

### 2.1 Experimental Setup and Measurements

Taking into account that soil moisture and temperature is distributed homogeneously in the probe, thermal conductivity ( $\lambda$ ) can be determined by Eq. 2.1:

$$\lambda = \frac{q}{4\pi\Delta T} \ln(t) + c \quad (2.1)$$

with  $\lambda$  thermal conductivity ( $\text{W}\cdot\text{m}^{-1}\cdot\text{K}^{-1}$ ),  $q$  Heat input rate ( $\text{W}\cdot\text{m}^{-1}$ ),  $T$  Temperature ( $^{\circ}\text{K}$ ),  $t$  Time (s), and  $c$  Constant.

When the increase of the soil temperature as a function of time is measured continuously, then soil thermal conductivity can then be predicted using Eq. 2.2:

$$\lambda = \frac{q}{4\pi S} + c \quad (2.2)$$

with  $S = \Delta T / \ln(t)$ .

In principle, the lab technique picks up the so-called HYPROP evaporation method developed by Schindler et al. (2010), as shown in Fig. 1. Since the water content  $\theta$  corresponding to  $\lambda$  Eq. 2.2) is based on the mass of the soil sample a linear distribution of  $\theta$  over the height of the sample is assumed. Schindler pointed out that the linearization error is negligible and concluded that the evapotranspiration method yields accurate values of soil hydraulic soil properties [17, 18].

Technically, the heat transfer analyzers ISOMET 2104 and ISOMET 2114 were used to measure soil thermal conductivity. Both units consist of a single

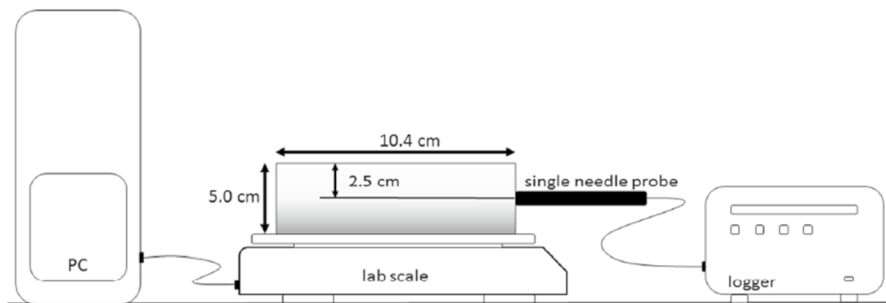
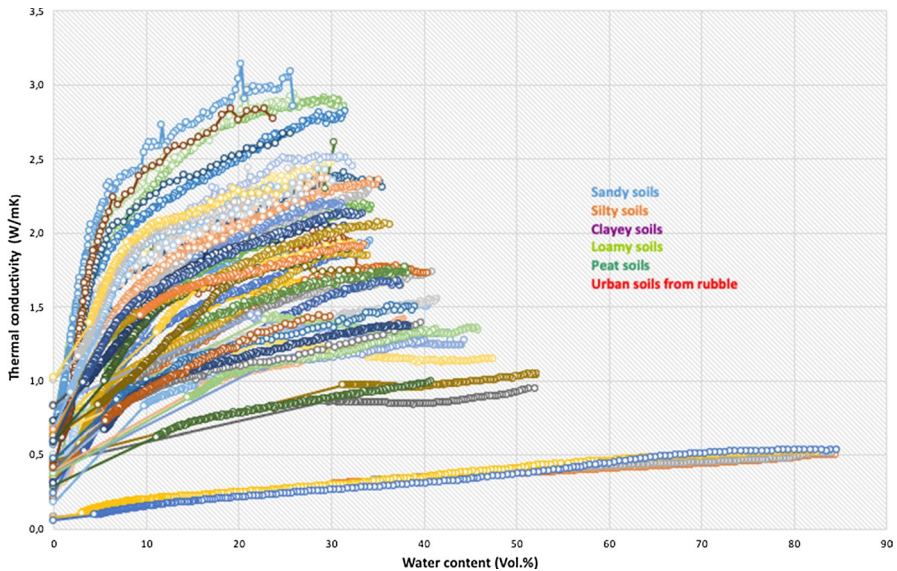


Fig. 1 Measuring device that has been used to determine the thermal conductivity of soils



**Fig. 2** Thermal conductivity for various soils as a function of the soil water content (Vol.%)

thermal needle probe and a measurement control device (data logger and PC). The needle probe has a length of 50 mm and 1.3 mm diameter. To insert the needle into the sample, a hole was carefully drilled with a special drill bit. According to the manufacturer,  $\lambda$  measurements can be carried out with an accuracy of about 10%. In order to raise up evaporation rate, a fan was additionally installed in most cases 30 cm above the sample. For all measurements plastic cylinders were used with a diameter of 10.4 cm, a height of 5 cm, and a volume of 425 cm<sup>3</sup>. Before measurements started, the cores were saturated by capillary rise on a ceramic plate. Afterward, the soil core is placed on a balance and the evaporation measurements start continuously. Records of the decreasing core weight starts from high to low water content at a lab temperature of 20 °C ± 2 °K. The interval for the individual thermal conductivity measurements was chosen to 30 min and for the water content records to 5 min. Whenever the water loss, i.e., evaporation rate was < 0.1 g·h<sup>-1</sup>, the experiment was terminated, and the sample was oven dried at 105 °C. After cooling to air temperature in a desiccator, bulk density and oven dry thermal conductivity were determined. For this purpose, the probe was reinserted into the existing borehole. Figure 2 shows the thermal conductivity loops at different water contents for > 60 soil cores with various textures and bulk densities.

In general, the thermal conductivity increases with the soil water content. However, the increase depends severely on soil texture and bulk density. A steep increase of the thermal conductivity with the amount of water content was observed for sandy and loamy soils, while it is less pronounced for silty soils, and even more for clayey soils. Organic soils such as peat soils are characterized by a very low thermal conductivity, which does not exceed 0.5 W·m<sup>-1</sup>·K<sup>-1</sup> even under wet conditions.

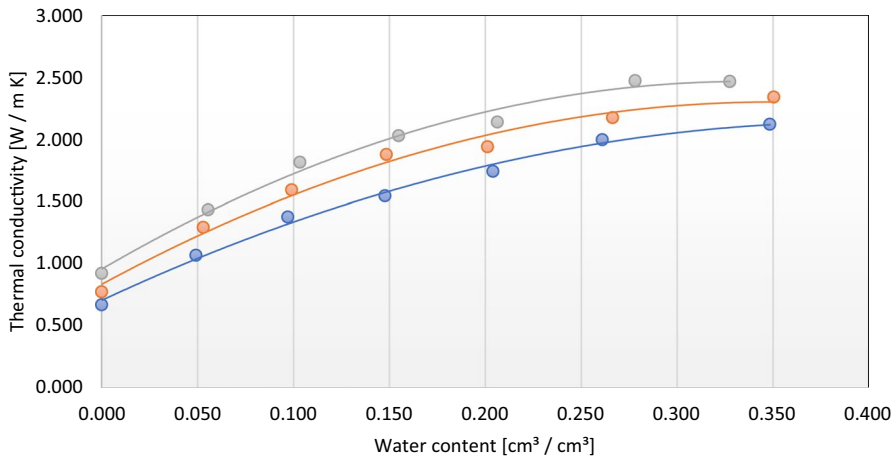


**Fig. 3** Influence of bulk density on the thermal conductivity of a loamy-silty sand for varying soil moisture conditions and bulk densities ( $\text{g cm}^{-3}$ ) of the dots in blue: 1.5, in red: 1.6, in gray: 1.8

Reasons of the high thermal variability within the same soil textural class are caused by differences in their mineral composition, bulk density, shape and size of particles, carbonate-, iron-oxide-, and soil organic matter content. The latter might also induce a partly water-repellent behavior of the soil particle surfaces leading to nonuniform moisture pattern during the drying-out process of the evaporation experiment. This water-repellent behavior might lead to an incomplete contact between needle and surrounding soil during the measurements. However, till today, there is no systematic study on how these factors influence the small-scale transport of heat, vapor, and water within the soil probe and lead at least to differences in thermal conductivity results.

Besides soil texture, also bulk density has a severe influence on the level of the thermal conductivity as shown exemplarily in Fig. 3 for a silty-loamy sand. In this example, the cores have been prepared and packed under controlled laboratory conditions.

Thermal conductivity in general rises with increasing bulk density. However, this effect also depends on the soil texture and mineral composition. The effect of an increasing thermal conductivity is mostly pronounced when the soil structure changes from a loosely to medium dense soil and reaches a maximum of water content  $> 30$  Vol.%.

## 2.2 Soil Data Base

The data set used is the result of uniform laboratory investigations within various research projects since 2010. Parental materials of 61 mineral soils with varying texture, 3 peat soils and 2 urban soils from rubble have been used for this study. The soils varied in texture, soil organic matter, carbonate, pH, and mineral composition. However, for the validation of the thermal pedo-transfer models, we standardized

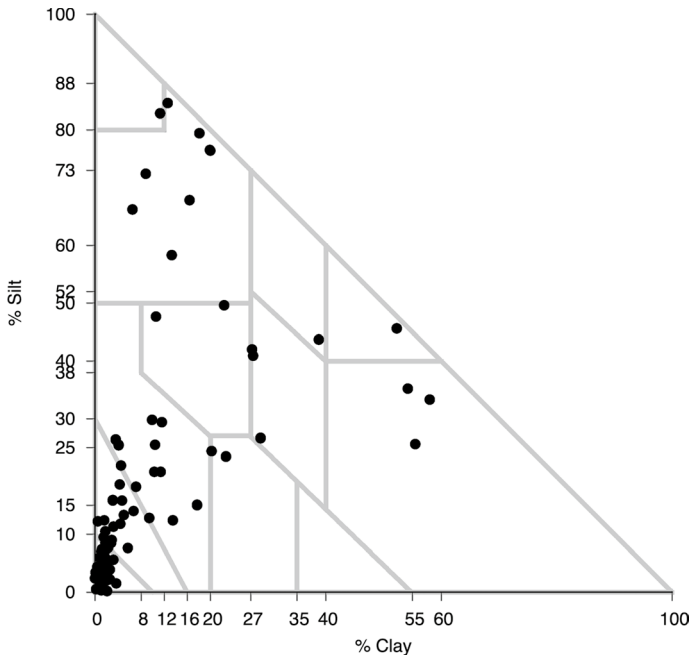


**Fig. 4** USDA-textural triangle position of all soils used in the data base

our data set: All in all, we used 2733 thermal conductivity measurements of 158 soil cores considering texture, bulk density, and the varying soil moisture only. Most (> 90%) of the soil samples were taken undisturbed in cylinders from an open soil profile. Only few, such as the urban soils, were taken as “disturbed samples” and prepared, i.e., homogenized and packed under controlled lab conditions. Figure 4 shows for all soils of the data base the classification within the USDA textural triangle. While sandy-, loamy-, and silty soils as well as transitional forms are represented well, there are only few clayey soils ( $n=5$ ) with > 35% clayey minerals.

Table 1 shows the results of a statistical analysis of the measurements. All results of the Shapiro–Wilk-test except the textural data result in a  $W$ -value close to 1, indicating a normal distribution of the data.

### 2.2.1 Thermal Conductivity Models to Be Validated

A large number of models have been developed to predict thermal conductivity mainly from soil bulk density and soil texture as described by Tarnawski et al. [11, 19, 20], and recently by He et al. [12]. Because the Quartz- content in soils is mostly not known, the sand content is often used as a proxy. Tarnawski et al. assessed the impact of quartz content on the prediction of soil thermal conductivity [20].

In this study, we focus on non-frozen soils only and tested all in all ten thermal conductivity models, i.e., pedotransfer functions. Based on the study and suggestions of He

**Table 1** Statistical analysis of the data base,  $n = 2733$

	$\lambda$ W·(mK)·h <sup>-1</sup>	$\theta$ %	Bulk density g·cm <sup>-3</sup>	Clay %	Silt %	Sand %
Minimum	0.23	0	1.03	0.0	0.2	2.1
1.Quantile	1.03	5.54	1.51	2.8	11.3	30.8
Median	1.52	15.1	1.61	9.4	20.8	70.4
Mean	1.51	16.2	1.60	12.2	27.2	60.8
3.Quantile	2.01	25.4	1.72	17.7	35.2	87.3
Maximum	3.08	50.6	1.91	58.0	84.6	99.3
<i>Shapiro–Wilk-test</i>						
<i>W</i>	0.985	0.949	0.978	0.775	0.775	0.883
<i>P</i>	<2.9e <sup>-16</sup>	<2e <sup>-16</sup>	<2e <sup>-16</sup>	<2e <sup>-16</sup>	<2e <sup>-16</sup>	<2e <sup>-16</sup>
Standard Deviation	0.624	12.0	0.172	13.4	24.1	31.5

et al. (2020), we only selected those, which have been qualified by the authors as "best performing" models.

Models may be grouped into physically based and purely empirical ones. Physically based models either try to calculate thermal conductivity from weighted averaging the thermal properties of soil constituents or they apply principles of percolation theory to heat flow in soil. Since physically based predictions of thermal conductivity do not include empirical parameters, they are expected to be applicable for a large range of soils. In contrast, empirical models may contain several empirical parameters. Some models use a nonlinear function to describe the whole range of thermal conductivity between saturation and dry soil. Moreover, Tarnawski et al. developed a temperature-dependent Kersten function [21]. For the most part, empirical models follow the idea of Kersten interpolating between dry soil thermal conductivity and its value at soil saturation [22]. Both of these boundary values must be known beforehand from empirical relations.

### 2.3 Physically Based Models

#### 2.3.1 The DeVries Method

DeVries calculates soil thermal conductivity from a volume-based weighted mean over all soil constituents [1]. To take into account the shape of soil mineral particles, an empirical parameter must be introduced. Above a certain threshold, water is assumed to be continuous, beneath of that threshold, soil air is regarded to be continuous. For further details readers are referred to Döll and her computer code "SUMMIT" to simulate the flow of heat and water beneath mineral liners of waste disposals [2]. The concept uses following equations:

$$\lambda(\Theta_L) = \frac{\sum k_i \Lambda_i \Theta_i}{\sum k_i \Theta_i} \quad \text{for } \Theta_L \leq \epsilon_k \tag{3.1}$$

**Table 2** Thermal conductivity  $\Lambda$  and shape factor ( $g_i$ ) of soil constituents after Döll with  $\Phi$  = porosity [2]

Soil constituent	i	$\Lambda_i$ W·m <sup>-1.0</sup> ·K <sup>-1</sup>	$g_i$
Water	1	0.57	–
Vapor and air	2	$\Lambda_{vapor} + \Lambda_{air}$	$0.035 + 0.298 \frac{\Theta_L}{\Phi}$
Quartz	3	8.8	0.125
Other minerals	4	2.0	0.125
Organic matter	5	0.25	0.5

$$\lambda(\Theta_L) = \lambda_{dry} + \frac{\lambda(\Theta_k) - \lambda_{dry}}{\Theta_k} \Theta_L \quad \text{for } \Theta_L < \epsilon_k \tag{3.2}$$

$\Lambda_i$  Thermal conductivity of soil constituent  $i$  (see Table 2),  $\Theta_i$  Volume of soil constituent  $i$  per unit soil volume,  $\Theta_L$  Volumetric water content,  $\Theta_k$  Threshold water content above which fluid phase is continuous.

$$\lambda_{dry} = 1.25 \frac{\Phi \Lambda_2 + \sum k_i \Theta_i \Lambda_i}{\Phi + \sum k_i \Theta_i} \tag{3.3}$$

$$k_i = \frac{2}{3} \frac{1}{1 + g_i \left( \frac{\Lambda_i}{\Lambda_1} - 1 \right)} + \frac{1}{3} \frac{1}{1 + \left( \frac{\Lambda_i}{\Lambda_1} - 1 \right) (1 - 2g_i)} \quad \text{for } i > 1, \quad \text{for } i = 1 \text{ holds } k_1 = 1 \tag{3.4}$$

Tian et al. and Tarnawski et al. recently picked up and modified the DeVries concept to estimate thermal conductivity of unfrozen and frozen soils [23, 24].

### 2.4 A Percolation-Based Effective-Medium Approximation: The Model of Sadeghi et al. (2018)

Percolation theory considers the formation of clusters under different conditions. To apply percolation theory to heat flow in partially saturated soils, the percolation-based effective-medium approximation (P-EMA) has shown to be useful Ghanbarian and Daigle. It allows the solid and the liquid phase to contribute simultaneously to heat flow [25]. In the framework of this approximation, a highly disordered medium is replaced by a uniform network whose effective conductivity is equal to the true conductivity of the real medium. Equations based on these concepts contain soil thermal conductivity implicitly. Sadeghi et al. (2018) developed an explicit formula to calculate soil thermal conductivity as a function of its water content [26]:



$$\Lambda = \left[ \frac{-(a_1 - \theta) + \sqrt{(a_1 - \theta)^2 - 4a_2a_3}}{2a_2} \right]^{t_s}, \quad \Lambda = \lambda^{(1/t_2)} \tag{3.5}$$

$$a_1 = \frac{\theta_c \lambda_{sat}^t - (\theta_s - \theta_c) \lambda_{dry}^t}{\lambda_{sat}^t - \lambda_{dry}^t} \tag{3.6}$$

$$a_2 = \frac{\theta_s - \theta_c}{\lambda_{sat}^t - \lambda_{dry}^t} \tag{3.7}$$

$$a_3 = \frac{-\theta_c \lambda_{sat}^t \lambda_{dry}^t}{\lambda_{sat}^t - \lambda_{dry}^t} \tag{3.8}$$

$$t = \frac{1}{t_s} \tag{3.9}$$

with  $\theta_c$  Critical water content,  $\theta_s$  Water content at saturation,  $t_s$  Scaling factor (fitted once and considered to be constant).

## 2.5 Non-linear Whole-Range Functions

### 2.5.1 The Model of Brakelmann

Brakelmann developed an empirical formula to estimate soil thermal conductivity based upon bulk density and water content [7]. His method has been used successfully for the planning of buried power cables:

$$\lambda = \lambda_w^\Phi \lambda_b^{(1-\Phi)} \exp(-3.08\Phi(1 - S)^2) \tag{3.10}$$

with  $\lambda_b$  thermal conductivity of soil mineral solids, approximated by:  $\lambda_b = 0.0812 * sand\% + 0.054 * silt\% + 0.02 * clay\%$ ,  $\rho_p$  particle density, approximated by

$$\rho_p = 0.0263 * sand\% + 0.0265 * silt\% + 0.028 * clay\% \tag{3.11}$$

Saturation degree,  $S = \theta / \Phi$ .

## 2.6 The Method of Lu et al. (2014)

Measured data of 17 mineral soils of contrasting properties were used to create a predictive model of soil thermal conductivity [27]. In this data set, all of the USDA texture classes are presented. Bulk density varies between 1.06 and 1.6 g cm<sup>-3</sup> and

organic matter content from 0.09 to 3.2%. To measure thermal conductivity, soil material was repacked into cores and moistened. The equations read:

$$\lambda(\theta) = \exp(\beta - \theta^{-\delta}) + \lambda_{dry} \tag{3.12}$$

$$\lambda_{dry} = 0.51 - 0.56\Phi \tag{3.13}$$

$$\delta = 0.67f_{clay} + 0.24 \tag{3.14}$$

$$\beta = 1.97f_{sand} + 1.87\rho_b - 1.36\rho_b f_{sand} - 0.95 \tag{3.15}$$

with  $f_{sand}$  sand content,  $\text{g g}^{-1}$  (0.063–2 mm),  $f_{clay}$  clay content,  $\text{g g}^{-1}$  (<0.002 mm).

The model comes with fixed parameter values which are assumed to be valid in all soils. Markert et al. picked up this approach to calibrate this model approach for three soil texture classes: sand, silt and silt [16]. Bertermann et al. finally used this approach for a comparison between measured and calculated thermal conductivities within different grain size classes [9].

## 2.7 Kersten Type of Prediction Methods

### 2.7.1 The Kersten Model (1949)

The Kersten number  $Ke$  represents a relative thermal conductivity which is defined by

$$Ke = \frac{\lambda - \lambda_{dry}}{\lambda_{sat} - \lambda_{dry}} \tag{3.16}$$

where  $\lambda_{dry}$  and  $\lambda_{sat}$  denote the thermal conductivity of dry and saturated soil, respectively, yielding

$$\lambda = \lambda_{dry} + Ke(S)(\lambda_{sat} - \lambda_{dry}) \tag{3.17}$$

where  $S$  is the saturation degree [22].

For interpolation purposes, Johansen et al. [27] proposed a normalized function  $Ke(S) = a + \ln(S)$ . Bertermann et al. recently advanced this approach for two soil textural classes, separated by 50% (silt + clay) [9].

$$\lambda = 0.1442(0.7\ln(\theta/\rho_b) + 0.4)10^{0.6243\theta} \tag{3.18}$$

While Eq. 3.18 is valid for soils containing >50% sand, Eq. 3.19 is referred to soils with <50% (silt% + clay%),

$$\lambda = 0.1442(0.9\ln(\theta/\rho_b) - 0.2)10^{0.6243\theta} \tag{3.19}$$

He et al., scrutinized a great number of pedo-transfer-functions to predict the thermal conductivity of soils [12]. Based on this study and suggestions, we selected those, which has been qualified by the authors as "best performing" models.

### 2.8 The Johansen Model (1977)

Johansen uses the basic Eq. (3.17) of all Kersten approximations [28]. He and coauthors estimated the thermal conductivity of natural dry soils by

$$\lambda_{dry} = \frac{0.135\rho_b + 64.7}{\rho_s - 0.947\rho_b} \tag{3.20}$$

For crushed rocks he proposes

$$\lambda_{dry} = 0.039\phi^{-2.2} \tag{3.21}$$

with  $\Phi$  porosity, approximated by  $\Phi = 1 - \rho_b / \rho_s$ .

The thermal conductivity of unfrozen soils at saturation is calculated by

$$\lambda_{sat} = \lambda_w^\phi \lambda_s^{(1-\phi)} \tag{3.22}$$

where  $\lambda_w = 0.57 \text{ W}\cdot\text{m}^{-1}\cdot\text{K}^{-1}$  denotes the thermal conductivity of water. The thermal conductivity of solids is approximated by

$$\lambda_s = \lambda_q^{\phi_q} \lambda_{other}^{(1-\phi_q)}$$

The index  $q$  stands for the quartz content, which thermal conductivity is assumed to be  $7.7 \text{ W}\cdot\text{m}^{-1}\cdot\text{K}^{-1}$ , while those of the other solids is set to  $2 \text{ W}\cdot\text{m}^{-1}\cdot\text{K}^{-1}$ . If the volume fraction of quartz is less than 20%, then the thermal conductivity of the other soil minerals is taken to be  $3 \text{ W}\cdot\text{m}^{-1}\cdot\text{K}^{-1}$ . According to Hu et al. [29], the volume fraction of quartz is assumed to be  $\phi_q = 0.5\phi_{sand}$ .

Between these two boundary values of  $\lambda_{dry}$  and  $\lambda_{sat}$ , thermal conductivity of unfrozen soils has to be interpolated by the formalism of Eq. 3.23

$$\text{if } S > 0.05, \text{ then } Ke = 1 + 0.7\log_{10}(S), \text{ else } Ke = 1 + \log_{10}(S) \tag{3.23}$$

For further details readers are referred to He et al. [12].

### 2.9 The model of Hu et al. (2001)

The model of Hu et al. [30], resembles that of Johansen except the Kersten coefficient which is given by

$$Ke = 0.9878 + 0.1811\ln(S) \tag{3.24}$$

To estimate the boundaries, Eqs. 3.20 and 3.21 are used with slightly changed constants which are  $\lambda_s = 3.35 \text{ W}\cdot\text{m}^{-1}\cdot\text{K}^{-1}$ ,  $\lambda_w = 0.6 \text{ W}\cdot\text{m}^{-1}\cdot\text{K}^{-1}$ , and  $\lambda_{air} = 0.0246 \text{ W}\cdot\text{m}^{-1}\cdot\text{K}^{-1}$

**Table 3** Coefficients of the Côté and Konrad model

Soil like materials	$k$
Gravel and coarse sand	4.6
Medium and fine sand	3.55
Silty and clayey soils	1.9
Organic fibrous soils	0.6

## 2.10 The Côté & Konrad model (2005)

Côté and Konrad [31] improved the Johansen model by introducing a coefficient  $k$  to account for the kind of soil material considered (Table 3).

Thus, the Kersten coefficient of this model yields from

$$Ke = kS[1 + (k - 1)S] \quad (3.25)$$

Further, they proposed to estimate thermal conductivity at the dry end using  $\lambda_{dry} = \chi 10^{-\eta\phi}$ . Here,  $\chi = 0.75$  and  $\eta = 1.2$  describe the average behavior of mineral soils. Côté & Konrad also studied crushed rocks and organic soils which are not in the focus of this study.

## 2.11 The model of Markle et al. (2006)

Following Ewen and Thomas [32] and Markle et al. [33], who proposed an exponential function to obtain  $Ke$  by

$$Ke = 1 - \exp(-\zeta S) \quad (3.26)$$

where  $\zeta$  represents a fitting parameter the value of which should be  $\zeta = 8.9$ . To obtain thermal conductivity, again Eqs. 3.17, 3.20, and 3.22 are used. For further details concerning the history of the method, readers are referred to He et al. [12].

## 2.12 The Model of Yang et al. (2005)

Yang et al. [34], introduced a new interpolation coefficient reading

$$Ke = \exp[k_T(1 - 1/S)] \quad (3.27)$$

which cannot be used down to  $S=0$ . The empirical coefficient  $k_T$  should be 0.36. While  $\lambda_{dry}$  is retained, the thermal conductivity at saturation is obtained from

$$\lambda_{sat} = 0.5^\phi (7.7^{\phi_{quartz}} 2^{1-\phi_{quartz}})^{1-\phi} \quad (3.28)$$

If the content of quartz is not measured, it can be estimated from sand content.

The focus of this study is not to qualify the transfer functions, but to give an overview on the performance using the data base.

**Table 4** Performance of ten pedo-transfer models for predicting soil thermal conductivity

Method	RMSE	COE	Bias	Correlation	Residual variance
deVries	0.342	0.933	0.01	0.780	0.341
Sadeghi	0.514	0.811	0.356	0.648	0.299
Brakelmann	0.384	0.902	-0.112	0.691	0.356
Kersten	1.051	0.695	-0.941	0.683	0.442
Lu et al	0.473	0.833	0.282	0.631	0.310
Johannsen	0.842	0.742	0.526	0.609	0.636
Hu	0.318	0.906	0.0871	0.799	0.194
Coté -Konrad	0.471	0.842	0.355	0.748	0.258
Markle	0.292	0.935	-0.019	0.782	0.256
Yang	0.643	0.607	-0.229	0.731	0.350

### 3 Testing and Validation

#### 3.1 Statistics

The above mentioned pedo-transfer models for estimating the thermal conductivity were applied to the data base described in chapter two. The goodness of fit was estimated on the basis of three criteria as suggested by Willmott et al. [35]. The Root Mean Square Error (RMSE), the bias, and the coefficient of efficiency are described by the following equations:

$$RMSE = \sqrt{\frac{\sum (y_i - \hat{y}_i)^2}{n}} \quad (4.1)$$

$$bias = \frac{\sum (y_i - \hat{y}_i)}{\sum y_i} \quad (4.2)$$

$$COE = 1 - \frac{\sum (\hat{y}_i - y_i)^2}{\sum} \quad (4.3)$$

Further, we set up a linear regression equation between measured and estimated values of thermal conductivity. Taking the residual variance into account, conclusions for further improvements might be possible.

#### 3.2 Results and Discussion

Table 4 summarizes the statistical performance of all models we used in our validation.

When a linear regression between measured values and calculation results is set up, the difference between its residual variance and RMSE indicates whether an improvement of the estimation method may be promising. This criterion suggests,

that the methods proposed by Sadeghi, Kersten, Lu, Hu, Coté & Konrad and Yang might be further rectified, although their regression equations are valid for the database currently used only. In Fig. 5, we present measured vs. predicted thermal conductivity data for five representative pedotransfer models.

Generally, one can conclude:

- All models follow more or less the 1:1 line, but with different degrees of data spreading and shifts
- The deVries physically based approach calculates  $\lambda$  quite well for all kind of soils, especially in the lower range  $< 1.5 \text{ W}\cdot\text{m}^{-1} \text{ }^\circ\text{K}^{-1}$ . However, its tendency leads to more under- and overpredictions in the high ranges of soil moisture.
- The same is true for the Brakelmann approach, which is solid and robust for all kind of soils. It mostly delivers trustful results till  $\lambda$  reaches a threshold of about  $2 \text{ W}\cdot\text{m}^{-1} \text{ }^\circ\text{K}^{-1}$ . Then, spreading increases, especially in the higher ranges of water content.
- The model of Lu clearly underestimates  $\lambda$  for about 0.5 to  $1.5 \text{ W}\cdot\text{m}^{-1} \text{ }^\circ\text{K}^{-1}$ .
- None of the Kersten-like models that have been qualified by He et al. [12], as “best suited ones” such as Johannsen, Hu et al., Côté/Konrad, and Yang, are better than the approaches of deVries or Brakelmann. Mostly, they underestimate  $\lambda$  in a range of  $0.5\text{--}1 \text{ W}\cdot\text{m}^{-1} \text{ }^\circ\text{K}^{-1}$ .
- Unexpectedly, the percolation theory, as described by Sadeghi et al. [26], does not lead to better prediction of  $\lambda$ .

All pedotransfer concepts tested here estimate the quartz content on the basis of the sand content. Because quartz has a strong influence on the soil thermal conductivity, it is recommended to adjust pedotransfer models regionally if the corresponding data are known and available. All in all, we suggest to collect more conductivity data for regional data validation scenarios.

Finally, in the next section we calculated guide values of the thermal conductivity for the USDA soil classes.

### 3.3 Estimation Frame of Thermal Conductivities for USDA Soil Classes

For many purposes in praxis, it is helpful and convenient to have guide values of the thermal conductivity. Since soil thermal conductivity depends on both, soil physical and mineral properties, and soil water content,  $\lambda$  is highly variable. However, for planning tasks it often needs standard values more than instantaneous values.

In order to meet this demand, we have created an estimation frame of thermal conductivity for various soils and bulk densities. Because these guide values are to be applied to very different soils, we consider it safer to use a physically based rather than an empirical method. Thus, we decided to take the deVries concept [1] as it was used in Döll [2] to set up an estimation frame for  $\lambda$ .

For this purpose, we first determined the center of each soil class in the USDA textural triangle and applied the pedo-transfer-function of Zacharias and Wessolek [36] to obtain

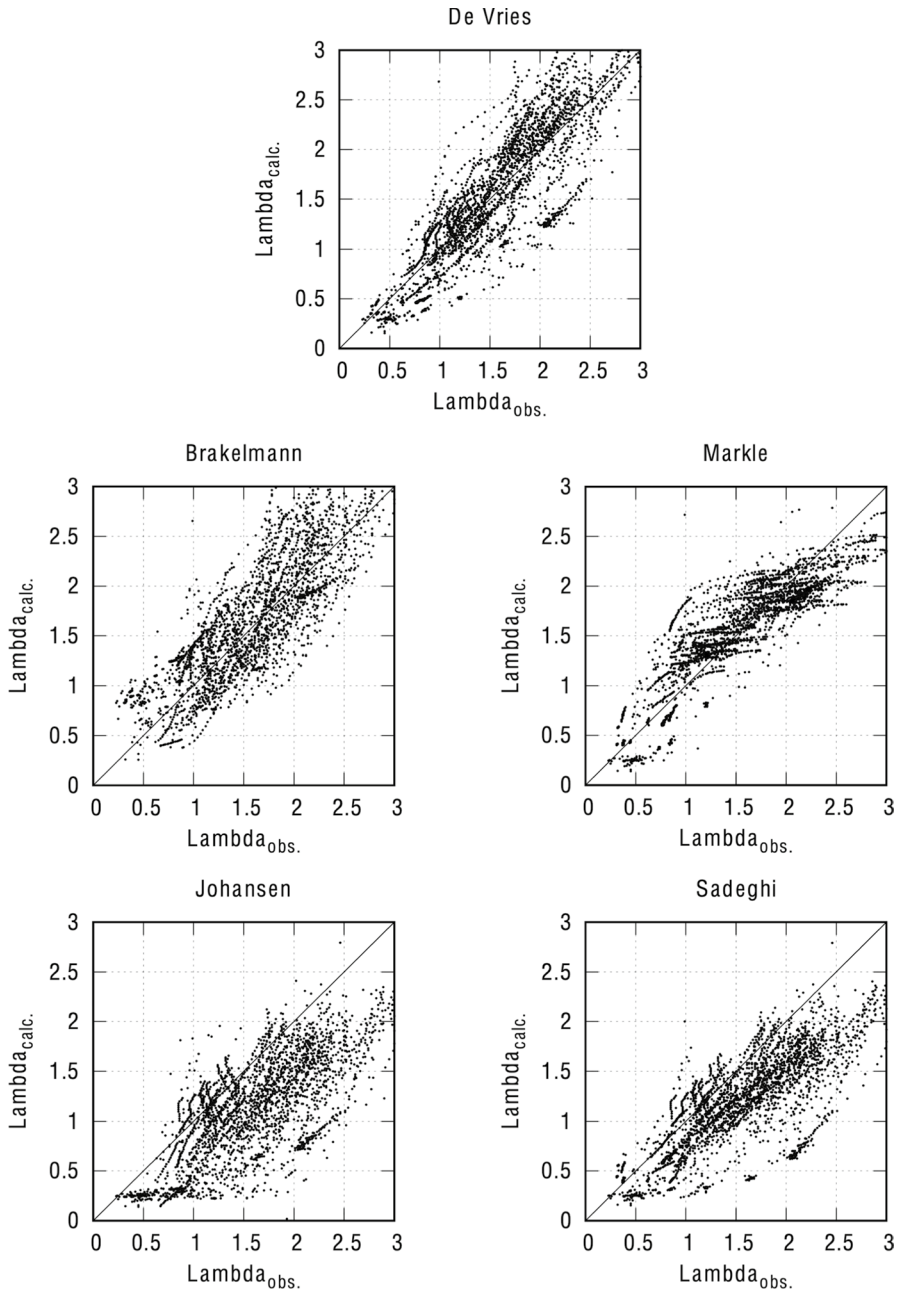


**Fig. 5** Measured vs. predicted thermal conductivity data ( $n=2733$ ) using the model approaches of deVries, Brakelmann, Markle, Johannsen, and Sadeghi

**Table 5a** Thermal conductivity  $W \cdot m^{-1} K^{-1}$  of the USDA soil texture classes, deVries method, bulk density:  $1.4 \text{ g} \cdot \text{cm}^{-3}$ , quartz content in sand and silt fraction: 90%, 50%, respectively ( $pF$  denotes the  $\log_{10}$  of tensiometer pressure, expressed in hPa)

IC	Texture class	$pF$									
		0.5	1.0	1.5	1.8	2.2	2.5	2.78	3.0	3.5	4.2
1	Sand	2.14	2.08	1.82	1.58	1.17	0.72	0.50	0.40	0.29	0.24
2	Loamy Sand	2.05	2.00	1.82	1.66	1.45	1.32	0.98	0.78	0.51	0.34
3	Sandy Loam	1.91	1.88	1.80	1.72	1.62	1.53	1.46	1.41	1.30	1.05
4	Loam	1.75	1.73	1.68	1.64	1.57	1.51	1.46	1.42	1.34	1.24
5	Silt	1.64	1.63	1.61	1.57	1.49	1.40	1.31	1.24	1.10	0.74
6	Silty Loam	1.67	1.66	1.63	1.59	1.52	1.46	1.41	1.36	1.27	1.16
7	Sandy Clayey Loam	1.79	1.77	1.70	1.66	1.60	1.55	1.51	1.47	1.40	1.32
8	Clayey Loam	1.60	1.58	1.55	1.52	1.47	1.43	1.40	1.37	1.32	1.25
9	Silty-Clayey Loam	1.52	1.51	1.49	1.46	1.42	1.39	1.36	1.34	1.29	1.22
10	Sandy Clay	1.68	1.05	1.59	1.56	1.51	1.48	1.44	1.42	1.37	1.30
11	Silty Clay	1.45	1.44	1.41	1.39	1.36	1.33	1.31	1.29	1.25	1.20
12	Clay	1.44	1.42	1.38	1.36	1.32	1.30	1.28	1.26	1.23	1.18

the parameters of the van-Genuchten-function (MvG). The advantage of this pedotransfer function is that it doesn't need any information on the soil organic matter content (SOM).

Following this pedo-transfer concept, one can easily calculate the thermal conductivity of each textural class for selected values of pressure head and bulk density. Results for three bulk densities ( $1.4, 1.6, 1.8 \text{ g} \cdot \text{cm}^{-3}$ ) are exemplarily shown in Table 5a, 5b, 5c.

Estimated Van Genuchten-Parameter of the USDA soil texture classes for a bulk density of  $1.4 \text{ g} \cdot \text{cm}^{-3}$ , calculated with a pedotransfer function after Zacharias and Wessolek,  $\theta_r = 0$  [36]

IC	$\theta_s$	$\alpha$	$n$
1	0.4339	0.0438	1.8363
2	0.4318	0.0465	1.5368
3	0.4249	0.0436	1.2478
4	0.4342	0.0356	1.1678
5	0.4187	0.0091	1.3734
6	0.4283	0.0182	1.2017
7	0.4448	0.0818	1.1328
8	0.4532	0.0523	1.1079
9	0.4524	0.0344	1.0998
10	0.4622	0.1294	1.1005
11	0.4682	0.0572	1.0747
12	0.4865	0.1568	1.0707



**Table 5b** Thermal conductivity ( $W \cdot m^{-1} \cdot K^{-1}$ ) of the USDA soil texture classes, bulk density:  $1.6 \text{ g} \cdot \text{cm}^{-3}$ , deVries method, quartz content in sand and silt fraction: 90%, 50%, respectively

IC	Texture class	$Pf$									
		0.5	1.0	1.5	1.8	2.2	2.5	2.78	3.0	3.5	4.2
1	Sand	2.56	2.51	2.24	1.98	1.37	0.86	0.61	0.50	0.37	0.31
2	Loamy Sand	2.44	2.39	2.20	2.04	1.81	1.52	1.13	0.91	0.61	0.42
3	Sandy Loam	2.28	2.27	2.21	2.15	2.04	1.96	1.87	1.81	1.68	1.38
4	Loam	2.06	2.05	2.02	1.98	1.92	1.86	1.81	1.77	1.67	1.56
5	Silt	1.91	1.91	1.90	1.88	1.22	1.75	1.66	1.59	1.43	1.01
6	Silty Loam	1.96	1.95	1.94	1.91	1.86	1.80	1.74	1.70	1.59	1.46
7	Sandy Clayey Loam	2.13	2.11	2.06	2.02	1.96	1.91	1.86	1.82	1.75	1.65
8	Clayey Loam	1.86	1.85	1.83	1.80	1.76	1.72	1.69	1.66	1.60	1.52
9	Silty-Clayey Loam	1.76	1.76	1.74	1.72	1.68	1.65	1.62	1.60	1.55	1.48
10	Sandy Clay	1.97	1.95	1.91	1.87	1.82	1.79	1.75	1.73	1.67	1.60
11	Silty Clay	1.67	1.66	1.64	1.62	1.59	1.57	1.54	1.53	1.49	1.43
12	Clay	1.66	1.64	1.61	1.59	1.56	1.53	1.51	1.49	1.45	1.40

**Table 5c** Thermal conductivity ( $W \cdot m^{-1} \cdot K^{-1}$ ) of the USDA soil texture classes, bulk density:  $1.8 \text{ g} \cdot \text{m}^{-3}$ , deVries method, quartz content in sand and silt fraction: 90%, 50%, respectively ( $pF$  denotes the  $\log_{10}$  of tensiometer pressure, expressed in hPa)

IC	Texture class	$pF$									
		0.5	1.0	1.5	1.8	2.2	2.5	2.78	3.0	3.5	4.2
1	Sand	3.07	3.01	2.75	2.48	1.59	1.03	0.75	0.62	0.48	0.41
2	Loamy Sand	2.91	2.86	2.68	2.51	2.26	1.72	1.30	1.06	0.73	0.53
3	Sandy Loam	2.72	2.71	2.68	2.64	2.55	2.46	2.38	2.31	2.16	1.79
4	Loam	2.42	2.42	2.40	2.37	2.32	2.27	2.22	2.17	2.08	1.95
5	Silt	2.23	2.23	2.23	2.22	2.19	2.14	2.07	2.00	1.83	1.37
6	Silty Loam	2.29	2.29	2.28	2.27	2.23	2.18	2.13	2.08	1.89	1.83
7	Sandy Clayey Loam	2.52	2.50	2.47	2.44	2.38	2.33	2.28	2.24	2.16	2.05
8	Clayey Loam	2.17	2.16	2.14	2.12	2.09	2.05	2.02	1.99	1.93	1.85
9	Silty-Clayey Loam	2.03	2.03	2.02	2.01	1.98	1.95	1.92	1.90	1.84	1.77
10	Sandy Clay	2.31	2.30	2.26	2.23	2.19	2.15	2.11	2.09	2.03	1.95
11	Silty Clay	1.91	1.91	1.89	1.88	1.85	1.83	1.81	1.79	1.75	1.70
12	Clay	1.90	1.90	1.87	1.85	1.81	1.79	1.77	1.75	1.71	1.66

Estimated Van Genuchten-Parameter of the USDA soil texture classes for a bulk density of  $1.6 \text{ g} \cdot \text{cm}^{-3}$ , calculated with a pedotransfer function after Zacharias and Wes-solek,  $\theta_r=0$  [36]

IC	$\theta_s$	$\alpha$	$n$
1	0.3691	0.0414	1.8363
2	0.3670	0.0440	1.5368
3	0.3714	0.0231	1.2478
4	0.3807	0.0189	1.1678
5	0.3652	0.0048	1.3734
6	0.3747	0.0097	1.2017
7	0.3913	0.0434	1.1328
8	0.3996	0.0277	1.1079
9	0.3989	0.0182	1.0998
10	0.4087	0.0687	1.1005
11	0.4146	0.0303	1.0747
12	0.4330	0.0832	1.0707

Estimated Van Genuchten-Parameter of the USDA soil texture classes for a bulk density of  $1.8 \text{ g} \cdot \text{cm}^{-3}$ , calculated with a pedotransfer function after Zacharias and Wesolek,  $\theta_r=0$  [36]

IC	$\theta_s$	$\alpha$	$n$
1	0.3043	0.0392	1.8363
2	0.3022	0.0416	1.5368
3	0.3179	0.0123	1.2478
4	0.3272	0.0100	1.1678
5	0.3117	0.0026	1.3734
6	0.3212	0.0051	1.2017
7	0.3378	0.0230	1.1328
8	0.3461	0.0147	1.1079
9	0.3454	0.0097	1.0998
10	0.3552	0.0364	1.1005
11	0.3611	0.0161	1.0747
12	0.3795	0.0442	1.0707

## 4 Conclusions

A wide data set of  $\lambda(\theta)$  curves of 61 parental soil materials has been used to validate various pedo-transfer function for predicting thermal conductivity. The  $\lambda(\theta)$  data show typical, texture dependent patterns: A slight to moderate change in slope from high to low water contents for silty, clayey, loamy soils, and Peat Soils, while sandy soils are more characterized by a moderate change in slope from high to intermediate water contents followed by a distinct decrease at dry conditions.

All in all, we used 2733  $\lambda(\theta)$  data sets in order to test physically based models and empirical ones.

Physically based models either try to calculate thermal conductivity from weighted averaging the thermal properties of soil constituents or they apply principles of percolation theory to heat flow in soil. Since physically based predictions of thermal conductivity do depend to a lesser degree on empirical parameters, they are expected to be applicable for a large range of soils. In contrast, empirical models contain several empirical parameters.

Comparing measured vs. predicted results, suitable, i.e., reliable pedo-transfer models are the DeVries model, and the Brakelmann approach. Even the latter is robust and suitable for all soil textures. Surprisingly, most of the Kersten-like models that have been qualified by He et al. as “best suited ones” such as Johannsen, Hu et al., Côté/Konrad, and Yang are not better suited. In contrast, the model of Markle et al. performs excellent in our investigation.

However, it's difficult to give a specific reason for these trends. In most tests of the models, the data set that has been used for developing, is divers, took non-uniform sources or methods, and the total amount of data often is poor.

By combining both, the pedo-transfer function of Zacharias & Wessolek [35] for predicting Mualem-vanGenuchten parameters, and the physically based model of deVries, it was possible to estimate for each USDA soil class the thermal conductivity for selected pressure heads and defined bulk densities. For large scale planning purposes, these estimates may be more practicable and valuable than single point values of  $\lambda$ .

**Acknowledgements** We would like to thank Michael Facklam, Reinhild Schwartengraber, and Dr Markus Gregor for their technical support, and the Technische Universität Berlin for carrying the publication costs. We are grateful to Barbara Bohne for her help in designing graphs.

**Author Contributions** Conceptualization, G.W. and K.B.; Methodology, K.B., G.W., and S.T.; Validation & Statistics, K.B. and G.W.; Formal Analysis, K.B. and G.W.; Investigation, G.W. and S.T.; Resources, G.W. and S.T.; Data Curation, G.W. and S.T.; Writing—Original Draft Preparation, G.W. and K.B.; Writing & Review, G.W. and K.B.; Visualization, K.B. and G.W.; Supervision, G.W.; Project Administration, G.W. and S.T.; Funding Acquisition, G.W.

**Funding** Open Access funding enabled and organized by Projekt DEAL. Investigations were funded within the German research projects “WindNODE” and “Miboka” by the Federal Ministry of Education and Research, Germany (BMBF), by the Federal Institute for Geosciences and Natural Resources (BGR, Hannover), and by the Landesamt für Bergbau, Geologie und Rohstoffe Brandenburg (LBGR).

## Declarations

**Conflict of interest** The authors declare no conflict of interest.

**Open Access** This article is licensed under a Creative Commons Attribution 4.0 International License, which permits use, sharing, adaptation, distribution and reproduction in any medium or format, as long as you give appropriate credit to the original author(s) and the source, provide a link to the Creative Commons licence, and indicate if changes were made. The images or other third party material in this article are included in the article's Creative Commons licence, unless indicated otherwise in a credit line to the material. If material is not included in the article's Creative Commons licence and your intended use is not permitted by statutory regulation or exceeds the permitted use, you will need to obtain permission

directly from the copyright holder. To view a copy of this licence, visit <http://creativecommons.org/licenses/by/4.0/>.

## References

1. D.A. De Vries, Thermal properties of soils, in *Physics of Plant Environment*. ed. by W.R. Van Wijk (Wiley, New York, 1963), pp.210–235
2. Döll, P., Modeling of moisture movement under the influence of temperature gradients: Desiccation of mineral liners below landfills. Doctoral Thesis TU Berlin, Bodenökologie und Bodengeneese, Heft 20, p. 251 (1996).
3. Döll, P., H. Stoffregen, M. Renger, G. Wessolek, R. Plagge (1997): Non-isothermal water and vapor movement below landfills: Laboratory experiments on and computer simulations of desiccation in mineral liners. In: August, H., Holzlöhner, U., Meggyes, T. (Eds.): *Advanced Landfill Liner Systems*. Thomas Telford, London, pp. 210–221 (1997) <https://doi.org/10.1680/all.25905.0021>
4. P. Oclon, M. Bittelli, P. Cisek, E. Kroener, M. Pilarczyk, D. Taler, R.-V. Rao, A. Vallati, The performance analysis of a new thermal backfill material for underground cable system. *Appl. Therm. Eng.* **108**, 233–250 (2016)
5. O.E. Gouda, A.Z. EL Dein, G.M. Amer, Effect of the formation of the dry zone around underground power cables on their ratings. *IEEE Trans. Power Delivery* **26**, 972–978 (2011)
6. E. Kroener, A. Vallati, M. Bittelli, Numerical simulation of coupled heat, liquid water and water vapor in soils for heat dissipation of underground electrical power cables. *Appl. Therm. Eng.* **70**, 510–523 (2014). <https://doi.org/10.1016/j.applthermaleng.2014.05.033>
7. Brakelmann, H., Physical principles and calculation methods of moisture and heat transfer in cable trenches. etz-Report 19, 93p. (1984), Berlin; Offenbach.
8. Campbell, G.S., Bristow, K.L., Underground power cable installations: Soil thermal resistivity, Tech. Rep., Decagon Devices, 17/02 (2010) [https://www.academia.edu/62984026/Underground\\_power\\_cable\\_installations\\_soil\\_thermal\\_resistivity](https://www.academia.edu/62984026/Underground_power_cable_installations_soil_thermal_resistivity)
9. D. Bertermann, J. Müller, S. Freitag, H. Schwarz, Comparison between measured and calculated thermal conductivities within different grain size classes and their related Depth ranges. *Soil Syst.* **2**, 50 (2018). <https://doi.org/10.3390/soilsystems2030050>
10. Y. Dong, J.S. McCartney, N. Lu, Critical review of thermal conductivity models for unsaturated soils. *Geotech. Geol. Eng.* **33**, 207–221 (2015). <https://doi.org/10.1007/s10706-015-9843-2>
11. V.R. Tarnawski, M.L. McCombie, W.H. Leong et al., Canadian field soils IV: modeling thermal conductivity at dryness and saturation. *Int J Thermophys* **39**, 35 (2018). <https://doi.org/10.1007/s10765-017-2357-9>
12. H. He, K. Noborio, M.F. Dyck, J. Lv, Normalized concept for modelling effective soil thermal conductivity from dryness to saturation. *Eur. J. Soil Sci.* **71**, 27–43 (2020). <https://doi.org/10.1111/ejss.12820>
13. D.A. De Vries, A nonstationary method for determining thermal conductivity of soil in situ. *Soil Sci.* **73**, 83–89 (1952). <https://doi.org/10.1016/j.jrmge.2015.03.005>
14. Trinks, S., Einfluss des Wasser- und Wärmehaushaltes auf den Betrieb erdverlegter Energiekabel, PhD Thesis, Technical University of Berlin, in German (2010). <https://api-depositonce.tu-berlin.de/server/api/core/bitstreams/661222a1-62c1-4177-8594-3322901c11db/content>
15. A. Markert, A. Peters, G. Wessolek, Analysis of the evaporation method to obtain soil thermal conductivity data in the full moisture range. *Soil Sci. Soc. Am. J.* (2015). <https://doi.org/10.2136/sssaj2015.09.0316>
16. A. Markert, K. Bohne, M. Facklam, G. Wessolek, Pedotransfer functions of soil thermal conductivity for the textural classes of sand, silt, and loam. *Soil Sci. Soc. Am. J.* (2017). <https://doi.org/10.2136/sssaj2017.02.0062>
17. U. Schindler, W. Durner, G. von Unold, L. Müller, Evaporation method for measuring unsaturated hydraulic properties of soils: extending the measurement range. *Soil Sci. Soc. Am. J.* **74**, 1071–1083 (2010). <https://doi.org/10.2136/sssaj2008.0358>
18. S. Iden, C.J. Blöcher, A. Peters, W. Durner, Numerical test of the laboratory evaporation method using coupled water, vapor and heat flow modelling. *J. Hydrol.* **570**, 574–583 (2019). <https://doi.org/10.1016/j.jhydrol.2018.12.045>
19. V.R. Tarnawski, W.H. Leong, A series-parallel model for estimating the thermal conductivity of unsaturated soils. *Int. J. Thermophys.* **33**, 1191–1218 (2012). <https://doi.org/10.1007/s10765-012-1282-1>

20. V.R. Tarnawski, T. Momose, W.H. Leong, Assessing the impact of quartz content on the prediction of soil thermal conductivity. *Geotechnique* **59**, 331–338 (2009). <https://doi.org/10.1680/geot.2009.59.4.331>
21. V.R. Tarnawski, W.H. Leong, K.L. Bristow, Developing a temperature-dependent Kersten function for soil thermal conductivity. *Int. J. Energy Res.* **24**, 1335–1350 (2000). [https://doi.org/10.1002/1099-114X\(200012\)24:15%3C1335::AID-ER652%3E3.0.CO;2-X](https://doi.org/10.1002/1099-114X(200012)24:15%3C1335::AID-ER652%3E3.0.CO;2-X)
22. Kersten, Miles S., Thermal Properties of Soils. University of Minnesota, Institute of Technology, Bulletin no. 28 (1949) <https://hdl.handle.net/11299/124271>
23. Z. Tian, Y. Lu, R. Horton, T. Ren, A simplified de Vries based model to estimate thermal conductivity of unfrozen and frozen soil. *Eur. J. Soil Sci.* **67**, 564–572 (2016). <https://doi.org/10.1111/ejss.12366>
24. V.R. Tarnawski, B. Wagner, W.H. Leong, M. McCombie, P. Coppa, G. Bovesecchi, Soil thermal conductivity model by de Vries: Re-examination and validation analysis. *Eur. J. Soil Sci.* **72**, 5 (2021). <https://doi.org/10.1111/ejss.13117>
25. B. Ghanbarian, H. Daigle, Thermal conductivity in porous media: Percolation-based effective-medium approximation. *Water Resour. Res.* **52**, 295–314 (2016). <https://doi.org/10.1002/2015WR017236>
26. M. Sadeghi, B. Ghanbarian, R. Horton, Derivation of an explicit form of the percolation-based effective-medium approximation for thermal conductivity of partially saturated soils. *Water Resour. Res.* **54**, 1389–1399 (2018). <https://doi.org/10.1002/2017WR021714>
27. Y. Lu, S. Lu, R. Horton, T. Ren, An empirical model for estimating soil thermal conductivity from texture, water content, and bulk density. *Soil Sci. Soc. Am. J.* **78**, 1859–1868 (2014). <https://doi.org/10.2136/sssaj2014.05.0218>
28. Johansen, O., Thermal Conductivity of Soils, Corps of Engineers U.S. Army, Cold Regions Research and Engineering Laboratory (Hanover, N.H), pp. 291 (1977) <https://apps.dtic.mil/sti/pdfs/ADA044002.pdf>
29. G. Hu, L. Zhao, X. Wu, R. Li, T. Wu, C. Xie, Q. Pang, D. Zou, Comparison of the thermal conductivity parameterizations for a freeze-thaw algorithm with a multi-layered soil in permafrost regions. *CATENA* **156**, 244–251 (2017). <https://doi.org/10.1016/j.catena.2017.04.011>
30. X.-J. Hu, J.-H. Du, S.-Y. Lei, B.-X. Wang, A model for the thermal conductivity of unconsolidated porous media based on capillary pressure-saturation relation. *Int. J. Heat Mass Transf.* **1**, 247–251 (2001)
31. J. Cote, M. Konrad, A generalized thermal conductivity model for soils and construction materials. *Can. Geotech. J.* **42**, 443–458 (2005). <https://doi.org/10.1139/t04-106>
32. J. Ewen, H.R. Thomas, The thermal probe - A new method and its use on an unsaturated sand. *Geotechnique* **37**, 91–105 (1987). <https://doi.org/10.1680/geot.1987.37.1.91>
33. J.M. Markle, R.A. Schincariol, J.H. Sass, J.W. Molson, Characterizing the two-dimensional thermal conductivity distribution in a sand and gravel aquifer. *Soil Sci. Soc. Am. J.* **70**, 1281–1294 (2006). <https://doi.org/10.2136/sssaj2005.0293>
34. K. Yang, T. Koike, B. Ye, L. Bastidas, Inverse analysis of the role of soil vertical heterogeneity in controlling surface soil state and energy partition. *J. Geophys. Res.* (2005). <https://doi.org/10.1029/2004JD005500>
35. C.J. Willmott, M. Scott, K. Matsuura, A refined index of model performance. *Int. J. Climatol.* **32**, 2088–2094 (2012). <https://doi.org/10.1002/joc.2419>
36. S. Zacharias, G. Wessolek, Excluding organic matter content from pedotransfer predictors of soil water retention. *Soil Sci. Soc. Am. J.* **71**, 43–50 (2007). <https://doi.org/10.2136/sssaj2006.0098>

**Publisher's Note** Springer Nature remains neutral with regard to jurisdictional claims in published maps and institutional affiliations.